Received: 1 July 2021 | Revised: 18 August 2021 | Accepted: 20 August 2021

DOI: 10.1002/nano.202100235

RESEARCH ARTICLE

nano select Open Access WILEY

Ultrasonic spray coating of polyethylenimine (ethoxylated) as electron injection and transport layer for organic light emitting diodes: The influence of layer morphology and thickness on the interface physics between polyethylenimine (ethoxylated) and the Al cathode

Inge Verboven | **Rachith Shanivarasanthe Nithyanandakumar** | **Melissa Van Landeghem** | **Hilde Pellaers** | **Bart Ruttens** | **Jan D'Haen** | **Koen Vandewal** | **Wim Deferme**

Hasselt University, Institute for Materials Research (IMO-IMOMEC), Wetenschapspark 1, Diepenbeek B-3590, Belgium

Correspondence
Inge Verboven and Wim Deferme, Hasselt University, Institute for Materials Research (IMO-IMOMEC), Wetenschapspark 1, B-3590 Diepenbeek, Belgium.
Email: inge.verboven@uhasselt.be; wim.deferme@uhasselt.be

Inge Verboven and Rachith Shanivarasanthe Nithyananda Kumar contributed equally to this study.

Funding information
BOF UHasselt, Grant/Award Number: BOF20DCOV09; FWO-Vlaanderen, Grant/Award Number: G043320N

Abstract

Modern lighting is expected to be light weight, flexible, efficient, non-expensive and environmentally friendly fabricated. Organic light emitting diodes (OLEDs) meet all these requirements and can be manufactured using inexpensive and roll-to-roll compatible printing techniques. They, however, often use low work function, highly reactive metals, such as barium and calcium to facilitate electron injection, deposited using expensive and non-continuous vacuum techniques. Efficient and stable alternatives can be found in the aliphatic amines, polyethylenimine (PEI) and polyethylenimine(ethoxylated) (PEIE), that shift the work function of aluminum favorably for electron injection. This work demonstrates ultrasonic spray coating of PEI(E) as electron injection and transport layer for OLEDs, reducing the work function of the aluminum cathode by 0.355 eV allowing a luminous efficacy comparable to that of the OLEDs using calcium/aluminum electrodes. Slightly higher luminous results are noted for the OLEDs with spin coated PEI(E), indicating that the surface morphology and thickness of the PEI(E) layer are crucial factors: ultrasonic spray coated PEI(E) layers have an increased overall thickness and surface roughness. This study shows the potential of ultrasonic spray coating and the suitability of PEI(E) as excellent electron injection and transport layer for OLEDs and paves the way towards fully spray coated OLEDs.

KEYWORDS
electron injection and transport layer, organic light emitting diodes, printing techniques, ultrasonic spray coating

1 | INTRODUCTION

Lighting is one of the bare necessities of life that advances-rapidly with technology and the needs of humankind. Nowadays it is expected to be light weight, flexible, highly efficient, non-expensive and fabricated in an environment friendly way. Organic light emitting diodes (OLEDs) are often considered to be the future in solid state lighting, meeting all these beneficial requirements and offering even more, such as surface light emission, a wide viewing angle and a high color contrast.[1] A typical OLED stack has following layers: a bottom electrode, a hole injection and transport layer (HIL/HTL), an organic emissive layer (EML) (small molecules or conjugated polymers), an electron injection and transport layer (EIL/ETL) and a top electrode.[2,3] A low DC voltage across the electrodes of the device initiates the process of charge injection, charge carrier transport, recombination, exciton formation and finally radiative and/or non-radiative relaxation and thus light emission. A low cost and ubiquitous mass production of these devices, however, requires a non-expensive and continues manufacturing, while nowadays OLED layers are deposited using high-cost techniques such as vacuum deposition or lab-scale techniques like spin coating.[4] Alternatively, OLEDs can be manufactured using printing techniques such as screen printing, inkjet printing, slot-die coating, blade coating, pad printing, gravure coating and spray coating.[5] These are all economically viable techniques that ensure continuous and environmentally friendly manufacturing owing to, amongst others, the possibility of using water or alcohol-based solvents and a reduction in waste. Several examples can be found in recent literature for example Jang et al. demonstrated a simple patterning method based on blade coating to deposit transparent polymer electrodes such as poly(3,4-ethylenedioxy-thiophene)/poly(styrene sulfonate) (PEDOT:PSS).[6] The poly(p-phenylene vinylene) (PPV) polymer Super Yellow (SY) was inkjet printed by Amruth et al. and ultrasonically spray coated as light emitting layer for polymer OLEDs.[7,8] Also inkjet printing of the silver back electrode has been demonstrated using SY as emissive layer.[9] Chung et al. presented high performance and flexible polymer OLEDs (PLED) with a gravure contact printed HIL/HTL PEDOT:PSS and light emissive polymer LUMATION Green 1300.[10]

However, not all materials grant themselves to be deposited easily using printing techniques. The EIL/ETL is generally composed of low work function materials for an efficient electron injection. Low work function alkaline earth metals like barium (Ba) or calcium (Ca) are vacuum deposited due to their high reactivity.[11] The latter also makes them highly susceptible to oxidation in ambient conditions, an important drawback for future applications. Furthermore, research indicates that sub monolayers of these materials cause quenching of the photoluminescence of organic materials.[12] Literature shows that efficient and stable solution processable substitutes can be found in the aliphatic amines, polyethylenimine (PEI) and polyethylenimine ethoxylated (PEIE). Stolz et al. combined spin coated PEI and PEIE layers with Ag electrodes and observed a work function shift of, respectively, 1.5 and 1.3 eV.[12] Besides enabling the necessary electron injection and transport, PEI(E) is easily synthesized, cost-effective and relatively chemically stable in ambient conditions up to 4 weeks.[12] Optimal results were found in literature for a PEI(E) layers with a thickness around 5-10 nm.[12–14] Other research illustrates that the primary device degradation mechanisms depend on the cathode material that is in direct contact with the PEI layer: a substantial difference in operational lifetime was found for Ag and Al with respectively lifetimes of more than 10 and 200 hours.[11] In addition to an improved electron injection Chiba et al. demonstrated OLEDs using solution-processed EILs containing lithium quinolate (Liq) and PEI with an enhanced device lifetime.[15] Zhou et al. extensively investigated the use of PEIE as an electron injection layer (EIL) and showed that PEIE reduces successfully the work function of metal oxides (ITO, FTO and ZnO), metals (Au, Ag and Al), PEDOT:PSS and even graphene.[16] However, the above-mentioned articles used spin coating as a deposition technique for the PEIE layers which does not allow roll-to-roll processing. Pioneering work was done by Falco et al. using spray coating to apply PEI thin films for fully sprayed organic photodiodes.[14]

This article presents a study in which PEI and PEIE were applied using the ultrasonic spray coating (USSC) technique, optimized as EIL/ETL for OLEDs and compared to OLEDs with Ca as EIL/ETL which is extensively used in literature and industry. Besides comparing the OLED's luminous performances, a complete optical, physical and electrical characterization of the spin coated and ultrasonically spray coated PEI(E) layers was performed as well. Furthermore, the thickness dependence of the PEI(E) layer on the device performance was investigated. USSC employs the ultrasonic atomization technology that has a unique advantage over conventional spray coating techniques as previously used by Falco et al. based on two key features: the generation of very small and homogenous droplets of an extremely narrow range diameter size (20 μm) and their gentle application on the substrate with minimum "bounce back."[17] It is a roll-to-roll compatible, low-cost and environmentally friendly (usage of water and alcohol-based solvents and low-waste) technique that is easily operatable and highly suited for large-surface, high-throughput OLED manufacturing. The challenge using this technique lies, however, in obtaining a homogenous

5-10 nm thick layer of PEI(E). The novelty of this work is the application of this high-end technique to apply PEI(E) as EIL/ETL layer for OLEDs reaching similar luminous efficacies as OLEDs with the thermally evaporated EIL/ETL Ca. Furthermore PEI(E) is ultrasonically spray coated in ambient conditions while Ca is thermally evaporated in a nitrogen environment to prevent fast degradation. This study demonstrates the capability of the ultrasonic spray coating technique and confirms the suitability of PEI(E) as an excellent alternative for alkaline earth metals as EIL/ETL for OLEDs and paves the way towards fully printed OLEDs. Furthermore, its application is not limited to OLEDs and could be used for other organic electronics such as organic photovoltaics (OPV) and photodetectors.

2 | RESULTS AND DISCUSSION

2.1 | Optimal spin coated and ultrasonically spray coated PEI(E)

First, the spin coated and ultrasonic spray coated PEI(E) layers were optimized until maximum values of the photometric quantities luminous flux and luminous efficacy were obtained. Figure 1 shows graphs of these quantities in function of the voltage and their comparison to the reference OLEDs with Ca as EIL/ETL. These results demonstrate that PEIE is clearly an excellent alternative for Ca. The highest luminous flux of 4.61 lumen (at 7 V) is obtained by the OLEDs with spin coated PEIE, followed by 3.65 lm for the OLEDs with Ca, a typical value for this type of devices.[18] Lower values are reached by the OLEDs with spin coated PEI of 2.23 lm, the OLEDs with ultrasonically spray coated PEIE of 1.32 lm and PEI of 0.48 lm. The graph of the luminous efficacy indicates that the OLEDs with spin coated PEIE (34.49 lm W^{-1} at 3 V and 10.80 lm W^{-1} at 7 V) and PEI (28.27 lm W^{-1} at 3 V and 11.67 lm W^{-1} at 7 V) have much higher values than the OLEDs with Ca (22.36 lm W^{-1} at 3 V and 9.12 lm W^{-1} at 7 V). The most important observation; however, is that the luminous efficacy of the OLEDs with ultrasonically spray coated PEIE (16.36 lm W^{-1} at 3 V and 8.97 lm W^{-1} at 7 V) is similar to that of the OLEDs with Ca. The OLEDs with ultrasonically spray coated PEI, however, show the lowest values for the luminous efficacy (8.88 lm W^{-1} at 3 V and 5.83 lm W^{-1} at 7 V). Since the results for both photometric quantities for the OLEDs with ultrasonically spray coated PEI are much lower than for the other OLEDs, the article will further focus on the PEIE layer and the OLEDs with PEIE as EIL/ETL.

To explain and understand the function of the PEIE layer and the result of using different application techniques and layer thicknesses, the spin coated and ultrasonically spray coated PEIE layers were subjected to a profound morphological investigation.

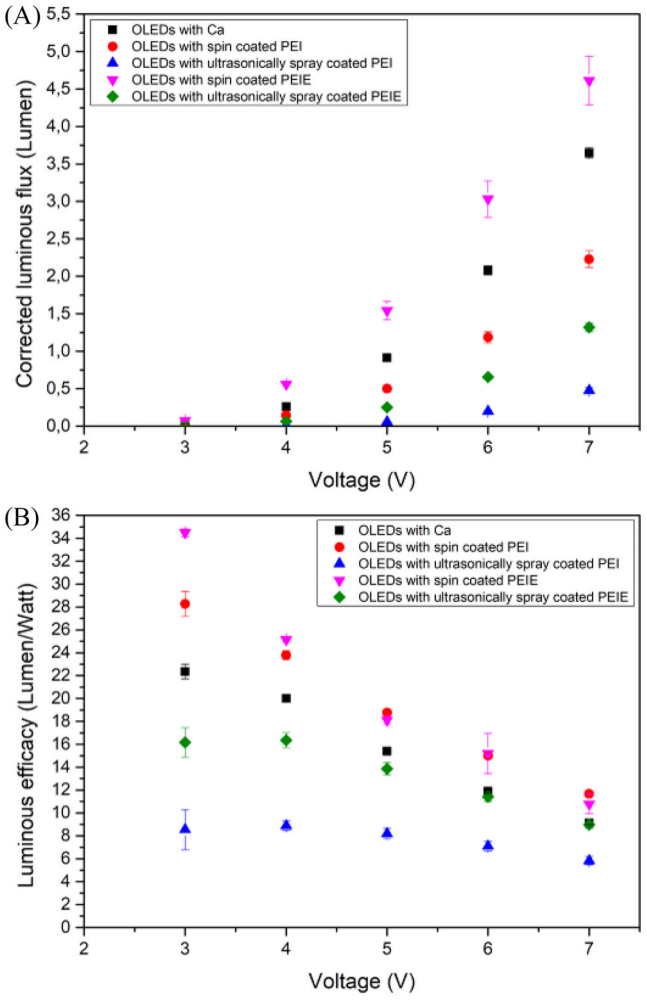

FIGURE 1 A), Luminous flux and B) luminous efficacy of OLEDs with Ca, PEI or PEIE as EIL/ETL

The surface morphology of an organic thin layer highly affects the electroluminescence properties and the devices performance; therefore, it is crucial for the proper functioning of the devices.[19] The layers have to possess a very smooth surface that can be expressed in a root mean square roughness (R_{RMS}) below 2 nm and a maximum roughness of the highest asperity (R_{max}) lower than 20 nm.[20] An AFM and SEM-EDX analysis was conducted to investigate the surface morphology and thickness of the optimal PEIE layer (5 layers with 0.4 mL min^{-1} flow rate). In order to conduct the AFM study, glass samples with spin coated and ultrasonically spray coated PEIE using the optimal coating parameters were fabricated. Figure 2 shows the results of this extended AFM investigation. It is apparent that the spin coated PEIE forms a more homogeneous layer with a lower roughness than the ultrasonically spray coated PEIE, which can be seen on both the surface AFM images (Figure 2A,C) and the 3D AFM

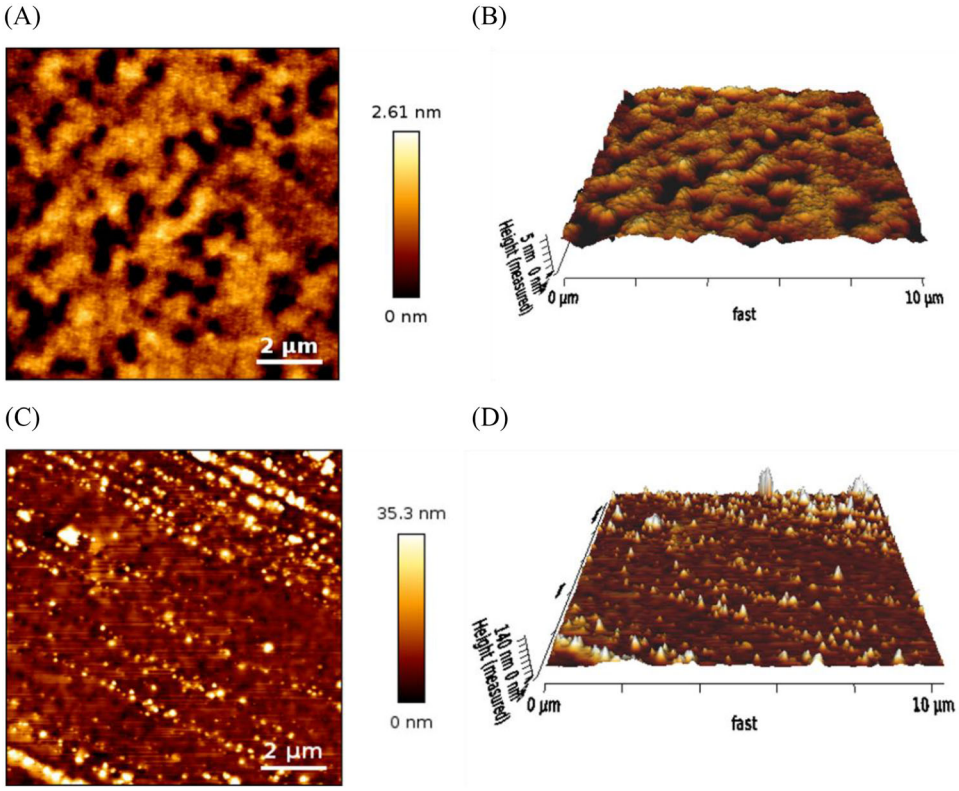

FIGURE 2 AFM images of glass with A) spin coated PEIE and C) ultrasonically spray coated PEIE and 3D AFM images of glass with B) spin coated PEIE and D) ultrasonically spray coated PEIE

images (Figure 2B,D). The spin coated PEIE layers seem to form worm-shaped agglomerations of the PEIE material, while in the ultrasonically spray coated PEIE layer high narrow agglomerations or peaks of different sizes are noticeable. Since an higher amount of passes with the ultrasonic spray nozzle leads to larger agglomerations, it might be the result of more PEIE material that is deposited using the ultrasonic spray coating technique. The average layer thickness for the measured spin coated PEIE was around 10 nm with a very small difference of less than 2 nm between the hills and valleys, which corresponds to the regularly indicated optimal layer in literature.[12–14] The ultrasonically spray coated layers show, however, a substantial difference in thickness between the different hills varying between 100 and 500 nm. The valleys show an average thickness of 10–30 nm. Initially, it was aimed to obtain ultrasonically spray coated PEIE layers with a thickness of 10 nm, but in order to achieve a fully closed PEIE layer, the layer thickness was increased. Lower PEIE layer thicknesses led to reduced luminous performances.

The formation of small agglomerations in the PEIE layer and the difference in layer morphology was confirmed by the SEM surface images in Figure 3. An ITO patterned glass substrate was applied with all OLED layers except for the Al contact such that the PEIE layer was the upper layer. The wavy line on the SEM images presents the transition of the glass sample with ITO (right) and without ITO (left). The spin coated PEIE establishes a homogeneous layer with evenly sized agglomerations (Figure 3A). The ultrasonically spray coated PEIE; however, forms an inhomogeneous layer with different sized agglomerations that seem to follow the pattern of the coffee ring effect (Figure 3B).[21]

SEM-EDX analyses, however, established the presence of PEIE in every section of the layers which is seen in Figure 4 that indicates the occurrence of nitrogen (N) on every investigated spot of the layers. This because N is only present in the PEIE and not in any of the underlying layers. From this, it can be concluded that both layers are closed layers that fully cover the sample with small imbedded islands or agglomerations.

These results show an important variation in layer morphology and thickness between PEIE applied by spin coating and by ultrasonic spray coating. This might be the most significant reason for the differences in device performance when comparing ultrasonically spray coated layers and spin coated ones. However, as discussed below, the difference in PEIE layer thickness also influences the work function reduction.

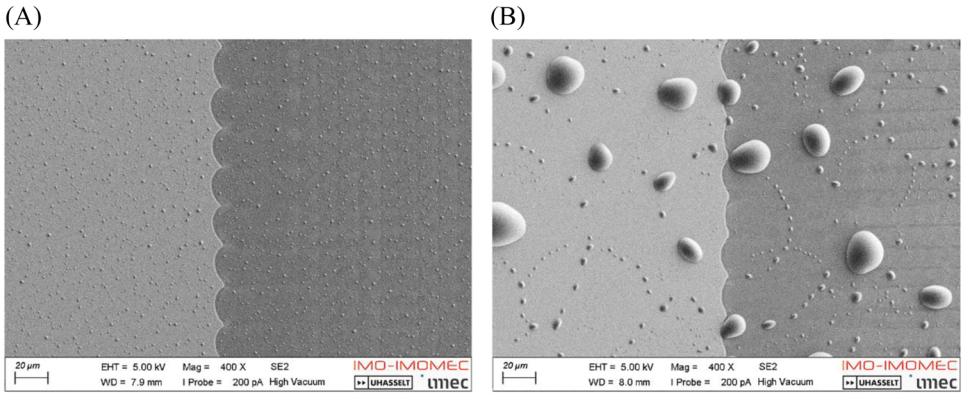

FIGURE 3 SEM surface images of samples with A) spin coated PEIE and B) ultrasonically spray coated PEIE

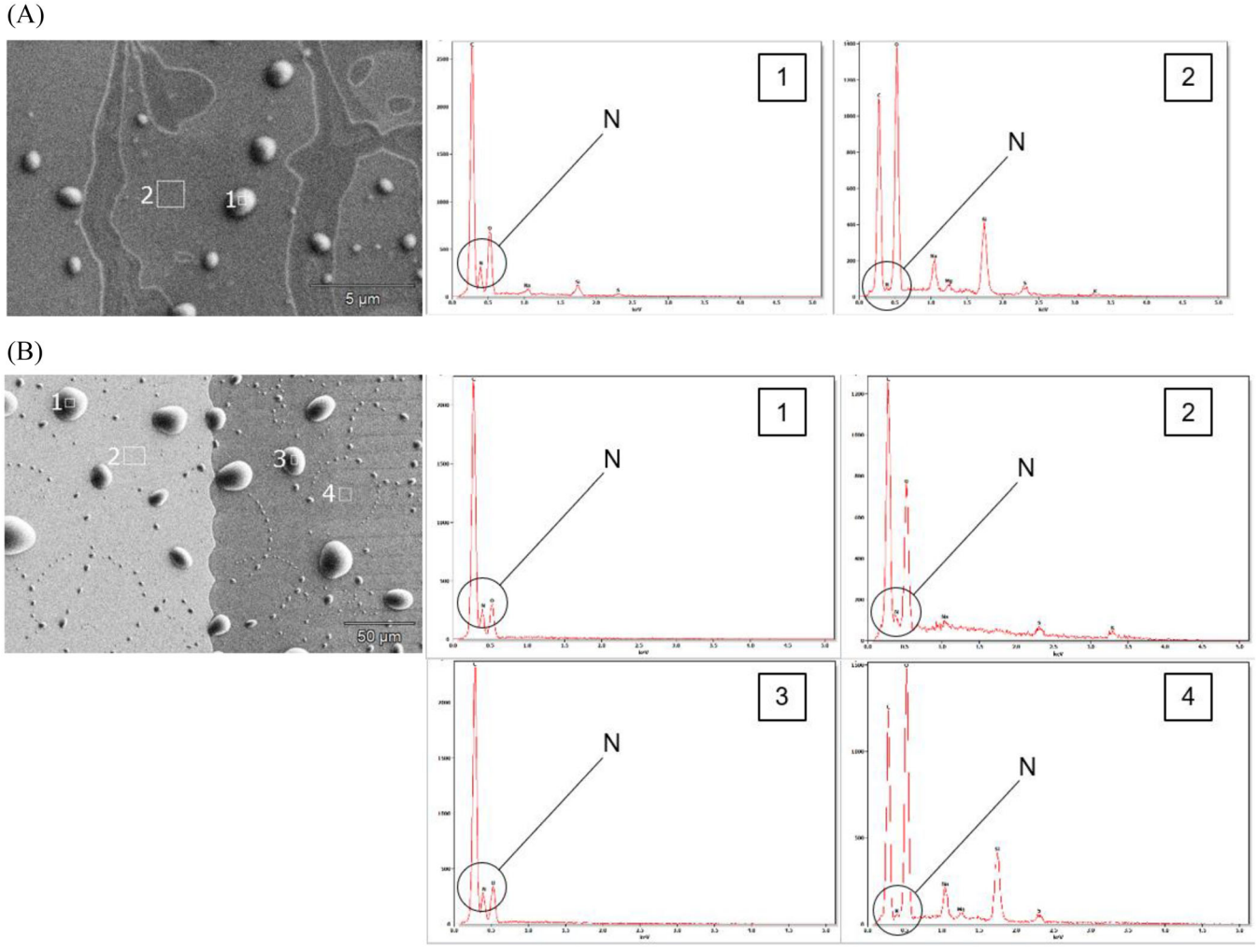

FIGURE 4 SEM-EDX analysis of samples with A) spin coated PEIE and B) ultrasonically spray coated PEIE

2.2 | Work function reduction mechanisms

PEIE is known to reduce the work function of the adjacent metal, Al in this case. When a metal is brought into contact with an organic layer it might arise in an energy level alignment at the organic-metal interface (for very thin organic layers) or in band bending in the organic layer (for thick organic layers that can be considered as bulk material).[22–24]

TABLE 1 Work function values found in literature for Ca and KPFM measured workfunction values for Al, Al/spin coated PEIE and Al/ultrasonically spray coated PEIE[25]

Materials	WF [eV]	WF reduction [eV]
Al	4.2	
Ca	2.9	
Al + SC PEIE	3.234	0.965
Al + USSC PEIE	3.845	0.355

Zhou et al. demonstrated that an energy level alignment at the organic semiconductor-metal interface takes place when an ultrathin layer of PEIE (1-10 nm) is physisorbed by the Al electrode.[16] A dipole surface layer is formed at the interface and the intrinsic molecular dipole moments of the neutral amine groups of PEIE induce a vacuum-level shift and therefore reduce the work function of Al and facilitate electron injection. This together with the hole blocking capabilities of PEIE leads to more efficient devices.[13] As thicker PEIE layers are applied, this material is more likely to function as an insulator with a band gap of 6.2 eV causing the device performance to be negatively affected.[16]

To investigate the work function reduction capabilities of the spin coated and ultrasonic spray coated PEIE on Al used in this work, Kelvin Probe Force Microscope measurements were conducted. For this purpose, 100 nm of Al was thermally evaporated onto glass samples followed by ultrasonically spray coated or spin coated PEIE. Table 1 shows the measured values for the work function. The work funtion reduction for the spin coated PEIE on Al samples is 0.965 eV and for the ultrasonically spray coated PEIE a value of 0.355 eV was measured. This correlates to a work function of Al reduced to 3.234 eV with the spin coated PEIE and to 3.845 eV with the ultrasonically spray coated PEIE. Ca, however, has a work function of 2.9 eV.[25] Using these measured values together with litterature values for SY allows to construct energy band diagrams of the full OLEDs shown in Figure 5.

For the spincoated PEIE there is no energy barrier to overcome for the electrons to be injected into the LUMO of the EML SY for the OLEDs.[26–29] The work function of Ca is lower than the LUMO level of SY implicating that it

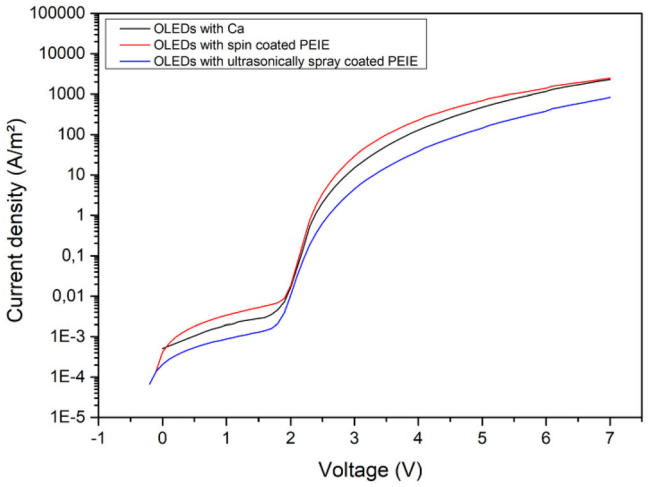

FIGURE 6 Current density (J-V) of OLEDs with Ca, spin coated PEIE and ultrasonically spray coated PEIE

is energetically favourable forelectrons to be injected from the Ca to the SY. On the other hand, the ultrasonically spray coated PEIE did not reduce the work function of Al enough so electrons and purely based on the kelvin probe measurements, it is expected that still a small energy barrier (0.6 eV) has to be overcome to enter the LUMO level of SY.

Both dipole formation and band bending might occur between the metal-organic interface or the PEIE-Al interface. The authors postulate that in the case of the thin spin coated PEIE layer, the formation of a dipole layer might take place, while band bending might happen for the ultrasonic spray coated PEIE layer. Both result in a reduction of the work function of the Al cathode. The spin coated layer could be seen as a surface modifer since it is physisorbed by the Al cathode, but the ultrasonically spray coated layer is thicker and therefore forms an actual layer. Since the latter is a thicker layer it is also more likely to function as an insulator.

To relate the KPFM measurements to electron injection into the devices, a comparison of the current density-voltage (J-V) characteristics of the devices with a Ca layer, a spin coated PEIE layer and an ultrasonically spray coated PEIE layer can be found in Figure 6. The OLEDs with

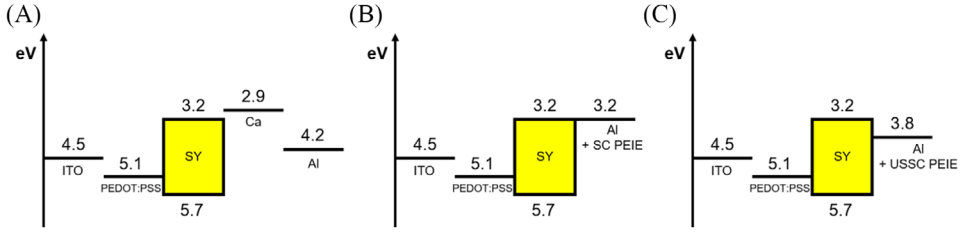

FIGURE 5 Energy band diagram of OLEDs with A) Ca, B) spin coated PEIE, and C) ultrasonically spray coated PEIE as EIL/ETL

spin coated PEIE show the highest current density at all voltages, followed by the OLEDs with Ca and finally the OLEDs with ultrasonically spray coated PEIE. This is consistent with the KPFM results: Current injection is indeed expected to be most efficient for the high work function metal Ca, followed by the lower work function PEIE/Al contact. In the latter case the junction between Al/PEIE and SY is that of a Schottky barrier allowing electrons to be injected efficiently through tunneling or thermionic injection.[12,16] The OLEDs with ultrasonically spray coated PEIE demonstrate the lowest current density, which is in line with all the above obtained results.

2.3 | Thickness and morphology dependence of PEIE layer

The proper functioning of the PEIE as surface modifier or actual electron injection and transport layer that reduces the work function of Al depends strongly on the PEIE layer thickness. Not only the mechanism at work to reduce the work function (energy level alignment or band bending) changes with layer thickness, but also the insulating capabilities of PEIE increase with layer thickness. In turn, the layer thickness also affects the morphology which, as stated above, should ideally be very smooth with a R_{RMS} below 2 nm and a R_{max} lower than 20 nm.[20] To investigate this layer thickness and morphology dependence of the PEIE layer, both the spin coated, and the ultrasonic spray coated layers were deposited at various thicknesses. For the spin coated samples, a higher concentration was used to achieve thicker layers of 45 and 80 nm (compared to the initial 10 nm). To ensure a significant difference in layer thickness, OLEDs were ultrasonically coated with 1, 5 and 10 layers of PEIE. Figure 7A,B compare the luminous flux and luminous efficacy for the fabricated devices. As expected, the OLEDs with a spin coated PEIE layer of 10 nm show the highest luminous flux, followed by the OLEDs with a spin coated PEIE layer of 45 nm. Although the devices with ultrasonically spray coated PEIE display minor differences between the luminous flux values, also here the same tendency can be found; the values decrease with increasing layer thickness. The devices with spin coated PEIE show similar values for the luminous efficacy for the different layer thicknesses of PEIE with slightly better results for the thinner layers. At the higher voltages (6-7 V) they seem to converge to the same value. An opposite trend can be noticed for the devices with ultrasonically spray coated PEIE, were the luminous efficacy rises with an increasing amount of PEIE layers. With an increasing amount of PEIE layers, the luminous flux differs only slightly as can be seen in Figure 7, but a larger decrease in current leads to a considerable rise in the luminous efficacy.

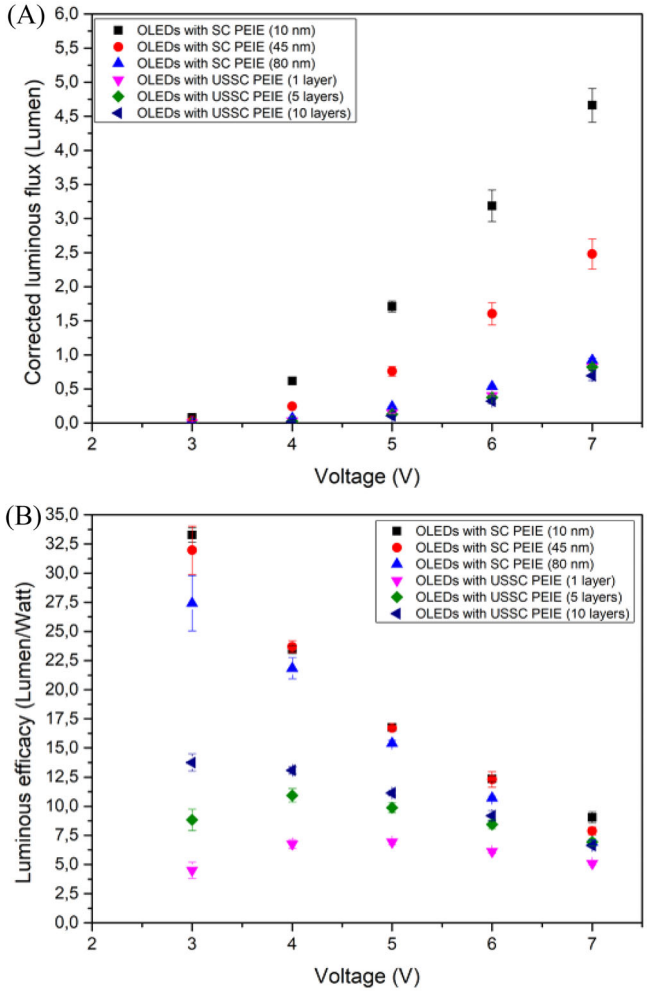

FIGURE 7 A), Luminous flux and B) luminous efficacy of OLEDs with spin coated and ultrasonically spray coated PEIE with different layer thicknesses

TABLE 2 KPFM measured work function values for Al, Al/spin coated PEIE and Al/ultrasonically spray coated PEIE with different layer thicknesses

Materials	WF [eV]	WF reduction [eV]
Al	4.2	
Al + SC PEIE (10 nm)	3.234	0.965
Al + SC PEIE (45 nm)	4.239	
Al + SC PEIE (80 nm)	4.292	
Al + USSC PEIE (1 layer)	3.817	0.383
Al + USSC PEIE (5 layers)	3.845	0.355
Al + USSC PEIE (10 layers)	4.190	0.01

Work function values were measured for all layers using a KPFM and displayed in Table 2. As expected, the samples with a spin coated PEIE layer of 10 nm show the highest work function reduction of almost 1 eV. The work function of Al is no longer being reduced for the samples with

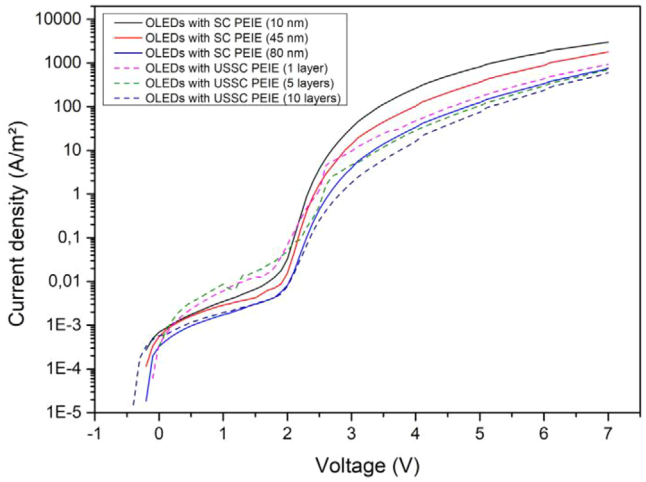

FIGURE 8 Current density (J-V) of OLEDs with spin coated and ultrasonically spray coated PEIE with different layer thicknesses

spin coated PEIE layers of 45 and 80 nm and for the OLEDs with ultrasonically spray coated PEIE with 10 layers. The samples with 1 and 5 layers of PEIE initiate a similar work function reduction of almost 0.4 eV.

It seems that pass a certain thickness of the PEIE layer, the work function of the Al cathode is not reduced anymore. Additionally, due to its low conductivity the thicker PEIE layers are more insulating. The electron injection is therefore expected to be less efficient for the thickest layers. Figure 8 shows the current density–voltage characteristics (J-V) of the OLEDs. As presumed the current density decreases when the PEIE layer thickness increases. As the PEIE layer thickness rises, less electrons can pass through the layer resulting in a lower current density. This is also confirmed by the results of the OLEDs with ultrasonically spray coated PEIE. Additionally, the tendency in the current density of the OLEDs with ultrasonically spray coated PEIE could also be the result of the amount of agglomerations, which is the lowest for the OLEDs with 1 layer of ultrasonically spray coated PEIE, resulting in the largest contact area and thus the highest current injection. Consequently, the lowest current density can be measured for the OLEDs with 10 layers of ultrasonically spray coated PEIE which have the smallest contact area due to the higher number of agglomerations.

The OLEDs with spin coated PEIE display a logical tendency for luminous flux and luminous efficacy; The highest results are found for the OLEDs with a 10 nm PEIE layer, while thicker PEIE layers leading to lesser results. All spin coated PEIE layers have the same homogenous surface morphology, hence the difference in performance can be primarily appointed to the difference in thickness.

As for the OLEDs with ultrasonically spray coated PEIE, the results and the corresponding explanation are more complex and demand further investigation. The highest electron injection and work function reduction of the Al cathode was found for the OLEDs with 1 PEIE layer, the lowest for the OLEDs with 10 layers PEIE. This same trend is noticed for the luminous flux, but the measured differences are so minor that the higher electron injection and thus higher current leads to an opposite trend in the luminous efficacy. Hence, the highest luminous efficacy was measured for the OLEDs with 10 PEIE layers and the lowest for the OLEDs with 1 PEIE layer. The ultrasonically spray coated layers, however, do not only differ in layer thickness, but also in surface morphology. SEM images in Figure 9 show clearly that the size of the agglomerations increases with an increasing number of layers spray coated layers. The rectangle in the left corner of the images is the patterned ITO.

An explanation for the tendency of the luminous efficacy to increase with number of spray coated layers might be found in these agglomerations that unintentionally created corrugated structures in the above lying Al cathode, enhancing scattering and light outcoupling.[30–33] To investigate whether this is the case, photoluminescence (PL) spectroscopy measurements were performed on the full OLED devices, as shown in Figure 10. However, no significant changes in PL intensity were observed. Moreover, the inhomogeneity of the luminescence within the active layer of a single device seems to be of similar magnitude as the variations between different devices as illustrated by the PL spectra of the device with 5 layers of PEIE recorded at two different positions. Hence, it is unlikely that increased light outcoupling due to scattering is the main cause for the enhanced luminous efficacy in the OLEDs with 5 and 10 layers of PEIE.

Another possible explanation might be found in the increased PEIE layer thickness that suppresses exciton quenching at the metal cathode.[34] An inserted EIL/ETL between the EML and the cathode with a thickness of approximately 30-40 nm could completely suppress quenching.[34] However, this mechanism of eliminating exciton quenching should also lead to an increased light output for the OLEDs with thicker spin coated PEIE layers, which is not the case as can be seen on Figure 7A. Interfacial degradation mechanisms might also contribute to the tendency of a decreasing luminous flux (Figure 7A) and current density (Figure 8), but an increasing luminous efficacy (Figure 7B) for the OLEDs with a rising number of ultrasonically spray coated PEIE layers. For organic/organic interfaces, thus, for the SY/PEIE interface, the interaction between accumulated charge carriers and excitons might result in exciton quenching and thus an increase in the OLED's driving voltages.[35–37] Similarly the organic/electrode interface, hence the PEIE/Al interface, is prone to degradation by excitons when they

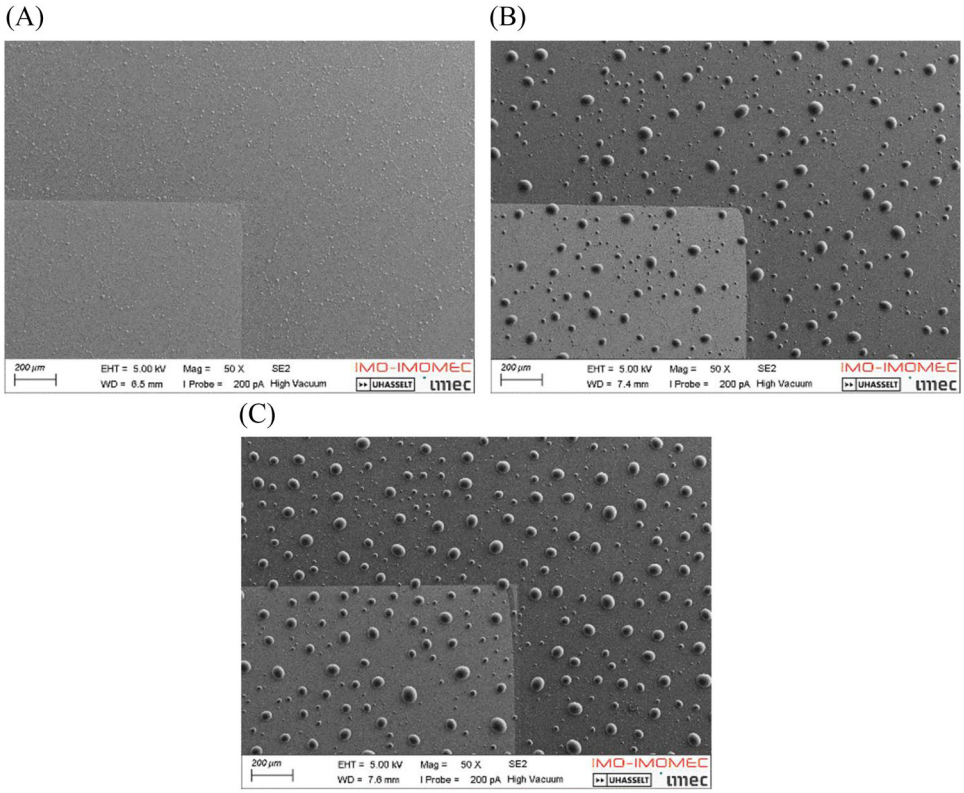

FIGURE 9 SEM surface images of OLED stack (without Al) with A) 1 layer, B) 5 layers and C) 10 layers of PEIE

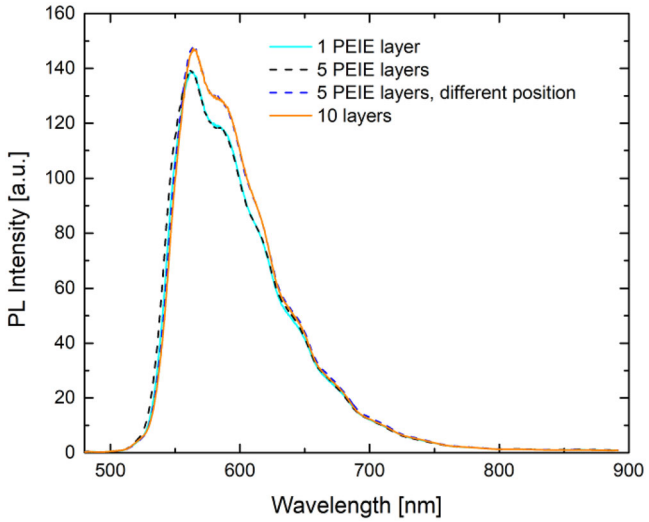

FIGURE 10 PL measurements on OLEDs with 1, 5, and 10 PEIE layers as EIL/ETL

reach the interface, which might result in a reduction in charge injection into the device and a decreased device efficiency.[38,39] Stolz et al. investigated the degradation mechanism of OLEDs with the similar device structure and discovered that exciton-induced degradation takes place at the SY/PEI/Al interface.[11] Possibly more excitons reach the PEIE/Al interface for the OLEDs with less PEIE layers leading to more exciton quenching.

It might also be suggested that the corrugated Al structures create or enhance plasmonic effects leading to improved luminous efficacies that manifest only under higher carrier densities.[40,41] Although, this seems less likely since an improved luminous efficacy is already noticeable at non-elevated charge carrier densities. The enhanced light output of the OLEDs with more PEIE layers or the reduced light output for the OLEDs with less PEIE layers cannot be linked directly to a single mechanism, but is probably due to a combination of all the above-mentioned processes.

3 | CONCLUSION

This study confirms the suitability of PEI(E) as an excellent alternative to the often-used alkaline earth metals like barium (Ba) or calcium (Ca) as EIL/ETL layer for OLEDs. Furthermore, these polymers can be applied using non-expensive, environmentally friendly and continuous manufacturing techniques such as ultrasonic spray coating. Ultrasonic spray coating allows for an adequate deposition of PEI(E) layers as EIL/ETL for OLEDs. The OLEDs with ultrasonically spray coated PEIE show lower values for the

luminous flux, but similar values for the luminous efficacy as the OLEDs where Ca is applied as EIL/ETL. This reduced luminous flux is due to the difference in surface morphology and the thickness of the PEIE layers. Agglomerations of material are formed in the ultrasonically spray coated PEIE layer that enlarge with an increasing layer thickness. The ultrasonically spray coated PEIE reduces the work function of the Al cathode by 0.355 eV and the spin coated PEIE causes a work function shift of 0.965 eV. The reduced work function of the Al cathode in the OLEDs with spin and spray coated PEIE leads to a more efficient electron injection resulting in improved OLED characteristics. To indicate the importance of the surface morphology and the thickness of the PEIE layers, different amounts of PEIE layers were spin coated and ultrasonically spray coated. When a certain layer thickness is reached the PEIE does not lower the work function of Al anymore and the electron injection into the device is reduced. It can therefore be stated that a thin spin coated PEIE layer is acting as a surface modifier, changing the work function and therefore enhancing electron injection. Although the ultrasonic spray coated PEIE layers also lower the work function of Al, the thicker PEIE layer somewhat hampers the electron injection. By further optimizing the surface morphology and reducing the layer thickness of the ultrasonic spray coated PEIE layers, the OLED characteristics will also improve and might even approach those of the OLEDs with spin coated PEIE. Non-invasive methods such as an additional buffer layer deposition and UV/ozone treatment could improve the surface roughness.[42,43] Another improvement can be made by adding zinc oxide (ZnO) nanoparticles to the PEI(E) solution in order to reduce the deterioration mechanism caused by excitons that reach and degrade the emitter/PEI(E) interface and enhance the device's performance.[11] This paper shows the potential of ultrasonic spray coating as a promising application technique to pave the way towards fully ultrasonically spray coated OLEDs.

4 | EXPERIMENTAL SECTION

4.1 | PEI and PEIE preparation and deposition

PEI and PEIE were applied as EIL/ETL by spin coating and ultrasonic spray coating. The PEI solution was prepared by dissolving PEI (Sigma Aldrich) in ethanol (EtOH) with a mass fraction between 0.05 and 0.4 wt%. Similarly, the PEIE solution was formulated with a mass fraction between 0.05 and 0.725 wt% of PEIE (80% ethoxylated, Sigma Aldrich) in isopropanol (IPA). Both solutions were briefly stirred before deposition. The PEI(E) solutions were spin coated at different rotational speeds and accelerations for 60 seconds to find the optimal layer thickness. Alternatively, the PEI(E) solutions were ultrasonically spray coated by varying multiple parameters to achieve an ultrathin homogeneous film. For these experiments an ultrasonic spray coater from Sono-Tek with impact nozzle was employed. This device utilizes ultrasonic atomization technology to deposit very small droplets of about 20 μm gently on a substrate (Figure 11). A high frequency electrical signal causes the mechanical expansion and contraction of two piezoelectric transducers, resulting in vibrations that are sent down the nozzle's horn, ultrasonically vibrating at the nozzles atomizing tip. The solution traveling to the center of the nozzle forms capillary waves due to this vibrational energy. When the solution emerges onto the atomizing surface, it reaches a critical wave amplitude and is broken down into a spray of tiny droplets by the ultrasonic energy concentrated here.

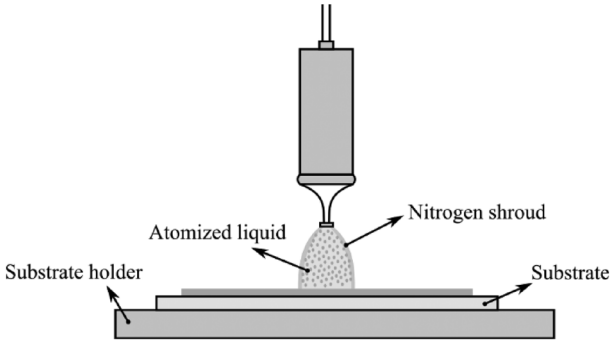

FIGURE 11 Ultrasonic spray coating. The atomization is realized by vibrations produced by the mechanical expansion and contraction of piezoelectric transducers inside the nozzle. A liquid that is fed into the devices forms capillary waves due to this vibrational energy. These waves emerge onto the atomizing surface where the kinetic energy is dissipated, and the liquid is broken down into a spray of micrometer sized droplets.

Different process parameters were tested to obtain an optimal layer of PEI(E) namely run power (RP), idle power (IP), nitrogen pressure (N pres), nozzle to substrate distance (NTSD), path speed (PS), hotplate temperature (HT), flow rate (FR) and number of passes (layers).[17] The run power is the power of the nozzle when operated. The idle power allows the nozzle to run at a reduced power when it is not spraying, locking on its frequency to ensure a better transition to the desired run power. Furthermore, it prevents clogging of un-atomized liquid inside the tip of the nozzle. The optimal parameters can be found in Table 3. As can be seen in the table the flow rate and the number of passes or layers varies to obtain an optimal PEI(E) layer. The thickness dependence of the PEI(E) layer will be discussed more in details in the discussion and conclusion sections.

TABLE 3 Ultrasonic spray coating parameters for optimized PEI and PEIE layers: Idle power (IP), run power (RP), nitrogen pressure (N pres), nozzle to substrate distance (NTSD), path speed (PS), hotplate temperature (HT), flow rate (FR) and number of passes (layers)

	Nozzle	IP [W]	RP [W]	N pres [psi]	NTSD [mm]	PS [mm s^{-1}]	HPT [°C]	FR [mL min^{-1}]	Layers
PEI	Impact	0.8	3	1.5	Std	2	30	0.2	4-7
PEIE	Impact	0.8	3	1.5	Std	2	30	0.3-0.4	1-10

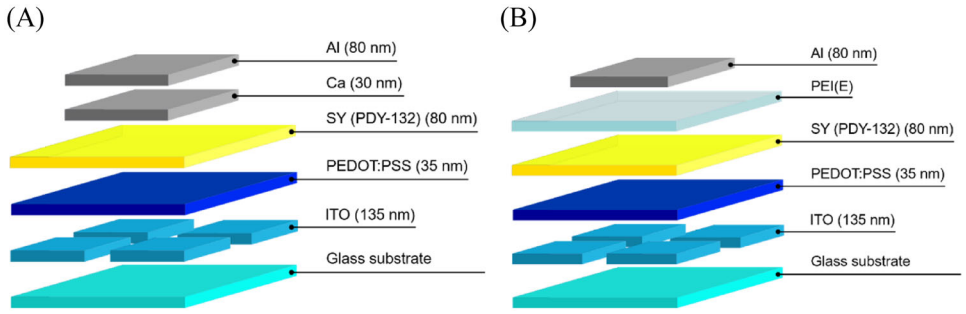

FIGURE 12 OLED device architecture on glass substrate with ITO anode, HIL/HTL PEDOT:PSS, EML SY and Al cathode and A) Ca as EIl/ETl and B) PEI(E as EIl/ETl

4.2 | OLED preparation and fabrication

Pre-patterned ITO glass substrates (Kintec, Kowloon, Hong Kong 150 nm, 20 Ω sq^{-1}) were soft cleaned prior to deposition by ultra-sonification in a soap solution (30 minutes), Milli-Q water (20 minutes), acetone (10 minutes) and isopropanol (IPA)(10 minutes) and dried with nitrogen. To complete the cleaning procedure and to increase the surface tension and therefore improve the wettability, the ITO substrates were UV ozone treated for 30 minutes.[44] The conductive polymer PEDOT: PSS (Heraeus, Hanau, Germany) was spin coated on top of the ITO anode as HIL/HTL at a rotational speed of 3000 rpm and an acceleration of 3080 rpm s^{-1} for 40 seconds. Prior to spin-coating the PEDOT:PSS dispersion was pressed through a chromafil 0.45 µm filter. After spin-coating a 15 minutes atmosphere annealing at 125°C was used and a film of approximately 35 nm film was obtained. This post-treatment dries and reduces the free volume between the polymer chain forming a crystalline and mechanically stable thin film.[40] The PPV-polymer Super Yellow (SY) (PDY-132, Merck, Darmstadt, Germany) was dissolved in chlorobenzene with a mass concentration of 5 mg mL^{-1} and stirred overnight at 50°C in an inert atmosphere glove box system (O2/H2O < 0.1 ppm). The solution was cooled down to room temperature and spin coated on top of the PEDOT:PSS with a rotational speed of 750 rpm and an acceleration of 500 rpm s^{-1} for 60 seconds, resulting in an emissive layer of about 80 nm. Subsequently a spin coated or ultrasonically spray coated PEI(E) layer was deposited on top as explained above. Finally, an Al cathode of 80 nm was thermally evaporated at a base pressure of 10^{-6} mbar. As reference, devices with thermally evaporated Ca (30 nm) as EIL/ETL instead of PEI(E) were also produced. Figure 12 shows the structure of the fabricate devices and their structure.

4.3 | PEI and PEIE film characterization

A complete optical, physical and electrical characterization of the ultrasonically spray coated PEI(E) layers was conducted. The surface morphology and thickness of the layers were examined using an atomic force microscope (AFM) of Bruker (Billerica Massachusetts, USA). In order to conduct this study, glass samples with spin coated and ultrasonically spray coated PEIE were fabricated using the optimal coating parameters. A scanning electron microscopy (SEM) with energy-dispersive X-ray spectroscopy (EDX) analysis was performed by employing a Zeiss 450 Gemini2 FEG-SEM (Carl Zeiss, Oberkochen, Germany). The detailed high resolution surface images produced by the SEM were used to investigate the layer morphology and the EDX provided elemental identification of the layer. For this purpose, PEDOT:PSS, SY and PEIE were sequentially applied on ITO patterned glass substrates (complete OLED stack without Al electrode). To determine the work function reduction of the Al cathode caused by PEI(E), frequency modulated Kelvin probe force microscopy (KPFM) (Park NX10, Park Systems, Mannheim, Germany) and with Pt/Ir coated tips (ST Instruments, Groot-Ammers, Nederland) was conducted.

Hereby, 100 nm of Al was thermally evaporated on glass substrates followed by ultrasonically spray coating or spin coating PEIE.

4.4 | OLED performance characterization

The produced OLEDs were measured using a Keithley 2401 source meter (Keithley Instruments, Cleveland, Ohio, USA) to obtain the current and voltage characteristics and by using an absolute calibrated integrating sphere spectrometer from Avantes (Apeldoorn, The Netherlands) to acquire the luminous flux. The luminous efficacy was then calculated by dividing the luminous flux by the used electrical power. Photoluminescence (PL) measurements were performed at room temperature with a 450 nm pulsed diode laser (Thorlabs, NPL45C, 6 ns pulse length) triggered by a function generator (Agilent 33220A) to operate at a pulse rate of 1 kHz. A polarizing filter reduced the average laser intensity to 0.25 μW, causing no observable sample bleaching during the experiments. PL collected in backscattering mode was diffracted in a grating spectrograph (Andor, Kymera 328i-D2-SIL) and registered by a linear back-illuminated CCD detector (Andor, iDus 416-LDC-DD). Spurious laser reflections were eliminated from the spectrum by means of a 450 nm band reject filter. In order to avoid photo-degradation, the devices were mounted in N_2 atmosphere in an airtight sample holder. All spectra were corrected for the spectral response of the set-up determined using a calibrated light source (Avantes, AvaLight-HAL-CAL-Mini).

ACKNOWLEDGMENTS

The authors would like to thank the financial contribution from BOF UHasselt (BOF20DCOV09) and FWO-Vlaanderen (project nr. G043320N).

CONFLICT OF INTEREST

We declare that this manuscript is original, has not been published before and is not currently being considered for publication elsewhere, either completely or in part, or in another form or language. No materials are reproduced from another source. We know of no conflicts of interest associated with this publication, and there has been no significant financial support for this work that could have influenced its outcome. As corresponding authors, we confirm that the manuscript has been read and approved for submission by all the named authors.

AUTHOR CONTRIBUTIONS

W. Deferme and I. Verboven designed and coordinated this research. W. Deferme supervised the work. R. S. Nithyanandakumar and I. Verboven performed the OLEDs processing and characterization. R. S. Nithyanandakumar conducted the AFM and KPFM measurements. M. Van Landeghem and K. Vandewal performed and analyzed the PL measurements. H. Pellaers, B. Ruttens and J. D'Haen performed the SEM/EDX analysis. W. Deferme, R. S. Nithyanandakumar and I. Verboven analyzed and interpreted all data. I. Verboven drafted the manuscript with aid from W. Deferme, R. S. Nithyanandakumar and M. Van Landeghem. All authors discussed the results and commented on the manuscript.

DATA AVAILABILITY STATEMENT

The data that support the findings of this study are openly available in Materials Cloud Materials Cloud repository at https://doi.org/10.24435/materialscloud:e6-sf.

ORCID

Inge Verboven https://orcid.org/0000-0003-3865-4766

REFERENCES

1. D. Chitnis, N. Thejo kalyani, H. C. Swart, S. J. Dhoble, *Renewable Sustainable Energy Rev.* **2016**, *64*, 727.
2. S. Chen, L. Deng, J. Xie, L. Peng, L. Xie, Q. Fan, W. Huang, *Adv. Mater.* **2010**, *22*, 5227.
3. S. Hofmann, M. Thomschke, B. Lüssem, K. Leo, *Opt. Express* **2011**, *19*, A1250.
4. A. Islam, M. Rabbani, M. H. Bappy, M. A. R. Miah, N. Sakib, *2013 Int. Conf. Informatics, Electron. Vis.* **2013**, *118*, 100760.
5. I. Verboven, W. Deferme, *Prog. Mater. Sci.* **2021**, *118*, 100760.
6. Y. Jang, J. Jo, D. S. Kim, *J. Polym. Sci. Part B Polym. Phys.* **2011**, *49*, 1590.
7. C. Amruth, M. Z. Szymański, B. Łuszczyńska, J. Ulański, *Sci. Rep.* **2019**, *9*, 1.
8. K. Gilissen, J. Stryckers, P. Verstappen, J. Drijkoningen, G. H. L. Heintges, L. Lutsen, J. Manca, W. Maes, W. Deferme, *Org. Electron.* **2015**, *20*, 31.
9. I. Verboven, J. Stryckers, V. Mecnika, G. Vandevenne, M. Jose, W. Deferme, *Materials*. **2018**, *11*, 290.
10. D.-Y. Chung, J. Huang, D. D. C. Bradley, A. J. Campbell, *Org. Electron.* **2010**, *11*, 1088.
11. S. Stolz, Y. Zhang, U. Lemmer, G. Hernandez-sosa, H. Aziz, *ACS Appl. Mater. Interfaces* **2017**, *9*, 2776.
12. S. Stolz, M. Scherer, E. Mankel, J. Schinke, W. Kowalsky, W. Jaegermann, U. Lemmer, N. Mechau, G. Hernandez-sosa, *ACS Appl. Mater. Interfaces* **2014**, *6*, 6616.
13. X. Yang, R. Wang, C. Fan, G. Li, Z. Xiong, G. E. Jabbour, *Org. Electron.* **2014**, *15*, 2387.
14. A. Falco, A. M. Zaidi, P. Lugli, A. Abdellah, *Org. Electron.* **2015**, *23*, 186.
15. T. Chiba, Y. Pu, T. Ide, S. Ohisa, H. Fukuda, *ACS Appl. Mater. Interfaces* **2017**, *9*, 18113.
16. Y. Zhou, C. Fuentes-Hernandez, J. Shim, J. Meyer, A. J. Giordano, H. Li, P. Winget, T. Papadopoulos, H. Cheun, J. Kim, M. Fenoll, A. Dindar, W. Haske, E. Najafabadi, T. M. Khan, H. Sojoudi, S. Barlow, S. Graham, J.-L. Brédas, S. R. Marder, A. Kahn, B. Kippelen, *Science (80-.).* **2012**, *336*, 327.

17. Sono-Tek Corporation, "*Ultrasonic spray coating," can be found under*. http://www.sono-tek.com/, **n.d**.
18. K. Gilissen, J. Stryckers, J. Manca, W. Deferme, *Proc. SPIE*, **2014**, 918311.
19. S. H. Lim, G. Y. Ryu, J. H. Seo, J. H. Park, S. W. Youn, Y. K. Kim, D. M. Shin, *Ultramicroscopy* **2008**, *108*, 1251.
20. E. P. Daniel J. Gaspar, *OLED Fundamentals Materials, Devices, and Processing of Organic Light-Emitting Diodes*, Taylor & Francis Group; *LLC*, **2015**.
21. R. D. Deegan, O. Bakajin, T. F. Dupont, *Nature* **1997**, *389*, 827.
22. M. Aoki, S. Toyoshima, T. Kamada, M. Sogo, S. Masuda, T. Sakurai, K. Akimoto, *J. Appl. Phys.* **2010**, *106*, 043715.
23. H. Ishii, K. Sugiyama, E. Ito, K. Seki, *Adv. Mater.* **1999**, *11*, 605.
24. B. S. Braun, W. R. Salaneck, M. Fahlman, *Adv. Mater.* **2009**, *21*, 1450.
25. S. M. Bouanati, N. E. Chabane Sari, S. Mostefa Kara, *Trans. Electr. Electron. Mater.* **2015**, *16*, 124.
26. S. R. Tseng, Y. S. Chen, H. F. Meng, H. C. Lai, C. H. Yeh, S. F. Horng, H. H. Liao, C. S. Hsu, *Synth. Met.* **2009**, *159*, 137.
27. B. H. J. Bolink, E. Coronado, J. Orozco, M. Sessolo, *Adv. Mater.* **2009**, *21*, 79.
28. S. Sapp, S. Luebben, Y. B. Losovyj, P. Jeppson, D. L. Schulz, A. N. Caruso, *Appl. Phys. Lett.* **2006**, *88*, 152107.
29. B. P. J. Hotchkiss, H. Li, P. B. Paramonov, S. A. Paniagua, S. R. Marder, S. C. Jones, N. R. Armstrong, J. Bre, *Adv. Mater.* **2009**, *21*, 4496.
30. M. M. Lu, *SID Symp. Dig. Tech. Pap.* **2013**, *44*, 912.
31. F. Löser, A. Haldi, J. Birnstock, F. Löser, T. Romainczyk, C. Rothe, D. Pavicic, A. Haldi, M. Hofmann, S. Murano, T. Canzler, J. Birnstock, *J. Photonics Energy* **2012**, *2*, 021207.
32. J. Feng, T. Okamoto, R. Naroaka, S. Kawata, *Appl. Phys. Express* **2013**, *93*, 051106.
33. W. H. Koo, S. M. Jeong, F. Araoka, K. Ishikawa, S. Nishimura, T. Toyooka, H. Takezoe, *Nat. Photonics* **2010**, *4*, 222.
34. A. L. Burin, M. A. Ratner, *J. Phys. Chem. A* **2000**, *104*, 4704.
35. H. Z. Siboni, H. Aziz, *Appl. Phys. Lett.* **2012**, *101*, 063502.
36. Q. Wang, H. Aziz, *Appl. Mater. Interfaces* **2013**, *5*, 8733.
37. Y. Zhang, Q. Wang, H. Aziz, *Appl. Mater. Interfaces* **2014**, *6*, 1697.
38. Q. Wang, G. Williams, T. Tsui, H. Aziz, *J. Appl. Phys.* **2012**, *112*, 064502.
39. Y. Zhang, M. M. A. Abdelmalek, Q. Wang, H. Aziz, *Appl. Phys. Lett.* **2013**, *103*, 063307.
40. M. L. Brongersma, N. J. Halas, P. Nordlander, *Nat. Publ. Gr.* **2015**, *10*, 25.
41. H. Yu, Y. Peng, Y. Yang, Z. Li, *NPJ Comput. Mater.* **2019**, *45*, 1.
42. C. P. Tan, H. G. Craighead, *Materials*. **2010**, *3*, 1803.
43. J. R. Vig, *J. Vac. Sci. Technol. B Microelectron. Nanom. Struct.* **1985**, *3*, 1027.
44. B.-S. Kim, D.-E. Kim, Y.-K. Jang, N.-S. Lee, O.-K. Kwon, Y.-S. Kwon, *J. Korean Phys. Soc.* **2007**, *50*, 1858.

How to cite this article: I. Verboven, R. S. Nithyanandakumar, M. Van Landeghem, H. Pellaers, B. Ruttens, J. D'Haen, K. Vandewal, W. Deferme, *Nano Select.* **2022**, *3,* 851.
https://doi.org/10.1002/nano.202100235